



# NIH Public Access

## Author Manuscript

*Cancer Res.* Author manuscript; available in PMC 2009 November 17.

Published in final edited form as:

*Cancer Res.* 2008 July 15; 68(14): 5733–5742. doi:10.1158/0008-5472.CAN-08-0190.

## Merlin Is a Potent Inhibitor of Glioma Growth

Ying-Ka Ingmar Lau<sup>1</sup>, Lucas B. Murray<sup>1</sup>, Sean S. Houshmandi<sup>2</sup>, Yin Xu<sup>1</sup>, David H. Gutmann<sup>2</sup>, and Qin Yu<sup>1</sup>

<sup>1</sup>Department of Oncological Sciences, Mount Sinai School of Medicine, New York, New York

<sup>2</sup>Department of Neurology, Washington University School of Medicine, St. Louis, Missouri

### Abstract

Neurofibromatosis 2 (NF2) is an inherited cancer syndrome in which affected individuals develop nervous system tumors, including schwannomas, meningiomas, and ependymomas. The *NF2* protein merlin (or schwannomin) is a member of the Band 4.1 superfamily of proteins, which serve as linkers between transmembrane proteins and the actin cytoskeleton. In addition to mutational inactivation of the *NF2* gene in NF2-associated tumors, mutations and loss of merlin expression have also been reported in other types of cancers. In the present study, we show that merlin expression is dramatically reduced in human malignant gliomas and that reexpression of functional merlin dramatically inhibits both subcutaneous and intracranial growth of human glioma cells in mice. We further show that merlin reexpression inhibits glioma cell proliferation and promotes apoptosis *in vivo*. Using microarray analysis, we identify altered expression of specific molecules that play key roles in cell proliferation, survival, and motility. These merlin-induced changes of gene expression were confirmed by real-time quantitative PCR, Western blotting, and functional assays. These results indicate that reexpression of merlin correlates with activation of mammalian sterile 20-like 1/2-large tumor suppressor 2 signaling pathway and inhibition of canonical and noncanonical Wnt signals. Collectively, our results show that merlin is a potent inhibitor of high-grade human glioma.

### Introduction

The most common brain tumor in adults is high-grade glial neoplasm, termed malignant glioma (1). Despite advances in neurosurgery, radiotherapy, and chemotherapy, the prognosis of malignant glioma remains dismal, with an estimated median survival of <1 year (2). With the emergence of biologically target-based therapies, it is important to identify new therapeutic targets and to develop novel targeted treatments to battle this deadly disease. Insights into the pathogenesis of gliomas are likely to arise from the study of inherited cancer syndromes, in which affected individuals are prone to the development of glial malignancies. One of these disorders is neurofibromatosis type 2 (NF2). Patients with NF2 develop schwannomas, meningiomas, and ependymomas, an uncommon type of glioma (3).

The *NF2* gene shares sequence similarity with the members of Band 4.1 superfamily (4,5). In particular, the *NF2* protein, merlin (or schwannomin), most closely resembles proteins of the ezrin-radixin-moesin (ERM) subfamily. Similar to the ERM proteins, merlin serves as a linker

---

©2008 American Association for Cancer Research.

**Requests for reprints:** Qin Yu, 16-20A-Icahn, 1425 Madison Ave, Department of Oncological Sciences, Mount Sinai School of Medicine, New York, NY 10029. Phone: 212-659-8218; Fax: 212-987-2240; qin.yu@mssm.edu.

**Note:** Supplementary data for this article are available at Cancer Research Online (<http://cancerres.aacrjournals.org/>).

**Disclosure of Potential Conflicts of Interest**

The authors have no conflicts of financial interest to declare.

between transmembrane proteins and the actin cytoskeleton and regulates cytoskeleton remodeling and cell motility (6–8). Unlike ERM proteins, merlin functions as a negative growth regulator or tumor suppressor. In this regard, mutational inactivation of the *NF2* gene is sufficient to result in the development of NF2-associated nervous system tumors. Moreover, *NF2* mutations have also been reported in other tumor types, including melanoma and mesothelioma (9), suggesting that merlin plays an important role, not only in NF2-associated tumors but also in sporadic cancers.

Merlin has a conserved trilobe NH2 terminal FERM (the band four-point-one/ezrin/radixin/moesin) domain, a central  $\alpha$ -helical region, and an extended COOH terminal tail (4,5). Merlin is capable of forming head-to-tail intramolecular and intermolecular association, and the head-to-tail closed conformation is required for the tumor suppressor activity (10,11).

Phosphorylation of Ser<sup>518</sup> at the COOH terminus results in an open conformation, which inactivates the tumor suppressor activity of merlin.

Whereas numerous studies have examined the role of merlin in schwannomas and meningiomas, comparatively little is known about the function of merlin in gliial cell tumors. In the present study, we show, for the first time, that merlin expression is dramatically reduced in high-grade human malignant gliomas. Furthermore, reexpression of merlin inhibits the growth of human glioma cells *in vitro* and *in vivo*, whereas *NF2* knockdown promotes glioma growth *in vivo*. Lastly, using microarray analyses and subsequent validation and functional assays, we show that merlin positively regulates the large tumor suppressor 2 (Lats2) signaling pathway and down-regulates canonical and noncanonical Wnt signaling. The demonstration that merlin is a critical negative regulator of glioma growth coupled with the identification of novel downstream effectors will provide new targets for the development of future brain tumor treatments.

## Materials and Methods

### Patient samples

The glioma tissue microarray was assembled at the M. D. Anderson Cancer Center, and additional tumor samples were obtained from the Washington University/Siteman Cancer Center Tumor Tissue Repository, as previously described (12). Human tissues were used in accordance with approved Human Studies Protocols.

### Cell lines and reagents

Human glioma cells, M089J, U138MG, DBRG05MG, LN229, M059K, Hs683, LN18, LN229, and A172 cells were obtained from American Type Culture Collection (ATCC); SNB19, U373MG, SF763, U251, SF268, SF539, U343MG, SF188, SF295, SF797, SNB75, SF126, SF210, U118MG, and U87MG and rat glioma cell 9L were obtained from University of California-San Francisco and National Cancer Institute (NCI). Normal human astrocytes (NHA cells) were obtained from ALLCELLS, Inc. Cells were maintained following the providers' and manufacturers' instructions. Anti-v5 epitope (Invitrogen), anti-merlin (Santa Cruz), anti-mammalian sterile 20-like 1/2 (MST1/2; Bethyl Laboratories), anti-Lats2 (Bethyl Laboratories), anti-Yes-associated protein (YAP; Abnova), anti-cellular inhibitor of apoptosis 1/2 (cIAP1/2; Santa Cruz), anti-actin (Sigma), anti-phosphorylated MST1/2 (Cell Signaling), anti-phosphorylated Lats2 (Abnova), and anti-phosphorylated YAP (Cell Signaling) were used in the experiments. 5-Bromo-2'-deoxy-uridine (BrdUrd) cell proliferation kit (Roche), Apoptag kit (Chemicon), and RhoA pull-down kit (Cytoskeleton, Inc.) were also used.

## Reverse transcriptase-PCR, mutagenesis, and expression and knockdown constructions

Full-length merlin isoform I was obtained as described (13), and the merlin mutants were generated using the QuikChange mutagenesis kits (Stratagene). Wild-type merlin and the merlin mutants together with their COOH terminal v5-epitope tags were cloned into the retroviral expression vector pQCXIP (BD Bioscience; ref. 13). Retroviruses were generated using these expression constructs and pVSVG/ GP2 293 cells following the manufacturer's instructions (BD Bioscience). All expression constructs were verified by DNA sequencing.

To knockdown merlin expression, several shRNAMir constructs against human merlin and a nontargeting shRNAMir control construct were obtained from Open Biosystems. Lentiviruses carrying these short hairpin RNAs (shRNA) were generated following the manufacturer's instructions.

## Lentivirus and retrovirus transduction

U87MG and U251 human glioma cells were first transduced with retroviruses carrying luciferase and a hygromycin-resistant gene and then transduced with retroviruses carrying the empty retroviral expression vector, wild-type merlin, or merlin mutants. RNA knockdown was accomplished using lentiviruses carrying shRNAs against merlin and a nontargeting control shRNA following the manufacturer's instructions. Infected cells were selected for their resistance to hygromycin and puromycin. Anti-v5 monoclonal antibody (mAb; Invitrogen) was used to detect exogenous merlin, whereas anti-merlin antibodies (Santa Cruz) were used for endogenous merlin.

## Expression profiling and real-time quantitative PCR

To compare gene expression profiles, we used human U133v2 gene chips (Affymetrix) and the probes derived from three independently transduced and pooled puromycin-resistant U87MG cells that reexpress merlin (U87MG<sub>merlin</sub>) or were transduced with empty retroviruses (U87MG<sub>wt</sub>) following standard protocols at the University of Pennsylvania Microarray Facility. Probe intensity data were imported to ArrayAssist Lite version 3.4 (Stratagene), and expression values for the probe sets were calculated using GCRMA. Affymetrix Absent, Marginal, and Present (A, M, P) scoring designations were also included. The data were then imported back to GeneSpringGX version 7.3.1 (Agilent) and filtered based on P in at least two of six samples. Finally, SAM version 2.2.1 (Stanford University) was applied using a two-class unpaired analysis, and differentially expressed genes were identified using a fold change cutoff of > 1.5 and a false discovery rate of <5%.

For patient sample analysis, cDNAs were prepared from 1 μg total RNA. Real-time quantitative PCR (qPCR) was performed and analyzed as previously described (12). In addition, total RNAs from U87MG<sub>merlin</sub> and U87MG<sub>wt</sub> cells were isolated using RNeasy columns (Qiagen). cDNAs were generated using SuperScript First-Strand Synthesis System for reverse transcription–PCR (Invitrogen). Primers for real-time qPCR were designed according to the Primer Bank Program (Massachusetts General Hospital<sup>3</sup>). qPCR was performed by using SYBR Green PCR Master Mix (Roche) and the Chromo4 real-time PCR Machine (Bio-Rad). The cycling variables used were 95°C for 8 min followed by 40 cycles of 95°C (15 s), 60°C (30s), and 72°C (30 s) and a melting curve analysis. Relative quantification of the targets were normalized with an endogenous housekeeping gene (TATA-box binding protein), and data analyses were performed using a comparative ( $\Delta\Delta Ct$ ) method using manufacturer's software and according to manufacturer's instructions.

<sup>3</sup><http://pga.mgh.harvard.edu/primerbank/index.html>

## Western blot analysis and immunocytochemistry

Cells and tumor samples were extracted with  $4 \times$  SDS Laemmli sample buffer without the dye, and protein concentrations were determined using Bio-Rad D<sub>c</sub> Protein Assay Reagents. For the immunocytochemical analyses, glioma cells were cultured in 35-mm dishes for 24 h and fixed in 3.7% paraformaldehyde. Fixed cells were then washed with PBS and blocked with 2% bovine serum albumin. Antibodies against v5-epitope or merlin were used to detect the appropriate antigens.

## Soft agar colony formation assays

To perform anchorage-independent growth assays, six-well plates were first covered with a layer of 0.6% agar made in 10% fetal bovine serum (FBS) DMEM and the pooled population of transduced U87MG cells ( $1 \times 10^5$  per well) in 0.3% agar (in DMEM) were seeded on top of the 0.6% agar layer and incubated in a humidified chamber for 3 wk. The six-well plates were inspected, and 30 randomly selected fields were photographed under a  $2.5 \times$  microscopic lens and a  $10 \times$  optical lens (25 $\times$  magnification). Colonies were then counted, and the mean number of colonies per field was calculated. All experiments were done in triplicate.

## Transwell tumor cell invasion assay

Tumor cell invasion assays were performed using Transwell chambers with 8- $\mu$ m pores (Costar) that were coated with a layer of Matrigel (Collaborative Biomedical). DMEM containing 10% FBS was added to the lower chambers of the Transwells. Transduced U87MG cells ( $2 \times 10^5$  per well) were seeded on the top of the Transwell in triplicate and incubated for 24 h. The bottom filters were fixed and stained at the end of the experiments. Cells in the top chambers were removed by wiping with cotton swabs, and the stained cells that had migrated through the Matrigel were counted under a microscope. Thirty randomly selected 100 $\times$  microscopic fields were counted.

## Apoptosis induced by chemotherapeutic drug and irradiation

Transduced U87MG cells were cultured with different concentrations of 5-fluorouracil (5-FU) (0, 5, or 50  $\mu$ mol/L; Sigma) and incubated at 37°C for 24 h. After the incubation period, the floating and adherent cells were harvested for apoptosis detection ( $n = 6$ ).

$4 \times 10^6$  transduced U87MG cells were irradiated by  $\gamma$ -radiation at a dose rate of 2.78 Gy/min and divided into sets that received 0, 5, 10, or 20 Gy of total irradiation. Irradiated cells were replated into culture dishes and incubated at 37°C for 2 d before harvest ( $n = 6$ ).

## Detection of apoptosis

Collected cells were lysed, diluted to  $10^4$  cells/mL in lysis buffer, and assayed for apoptosis using the Cell Death Detection ELISA kit (Roche), according to the manufacturer's instructions.

## Luciferase reporter assay

To measure canonical Wnt signaling in U87MG<sub>WT</sub> and U87MG<sub>merlinS518D</sub>, U87MG<sub>merlin</sub>, and U87MG<sub>merlinS518A</sub> cells, we used the  $\beta$ -catenin-responsive luciferase reporter construct (TopFlash, Addgene), which contains T-cell factor/lymphocyte enhancer factor (TCF/LEF) binding sites and a negative control construct, FopFlash, which contains mutated TCF/LEF binding sites. These reporters were transfected transiently into these transduced glioma cells in triplicate. The luciferase activity in these transfected cells were measured 24 h posttransfection following the manufacturer's instructions (Promega) using a Modulus Microplate Luminometer/Fluorometer (Turner Biosystems).

## Subcutaneous and intracranial tumor growth experiments

Pooled populations of transduced U87MG and U251 glioma cells were used for subcutaneous tumor growth experiments. Briefly,  $1 \times 10^6$  glioma cells were injected into each immunocompromised B6.129S7-Rag1<sup>tm1Mm</sup> (Rag1, Jackson Laboratories) mouse. Six mice were used for each type of the infected glioma cell lines. After solid tumors became visible (10–15 d after the injection), the longest and shortest diameters of the solid tumors were measured using a digital caliper every third day for 5 to 7 wk. Tumor volumes were calculated using the following formula: tumor volume =  $1 / 2 \times (\text{shortest diameter})^2 \times \text{longest diameter}$  ( $\text{mm}^3$ ). At the end of the experiments, tumors were fixed and sectioned for the histologic and immunologic analyses.

Transduced U87MG and U251 cells were also used for the intracranial tumor growth experiments. U87MG ( $2 \times 10^5$  cells in 10  $\mu\text{L}$  HBSS/Rag1 mouse)/U251 cells ( $1 \times 10^5$  cells in 10  $\mu\text{L}$  HBSS/Rag1 mouse) were stereotactically injected at the bregma 2 mm to the right of the sagittal suture and 3 mm below the surface of the skull. After injection, mice were closely monitored and the duration of their survival was recorded. Mice that showed signs of morbidity were euthanized and considered as if they had died on that day, and the number of surviving mice was recorded. The survival rates were calculated as follows: survival rate (%) = (number of mice still alive / total number of experimental mice)  $\times 100\%$ . At the end of the experiments, the mouse brains were removed, fixed, and sectioned for histologic analysis. Mice that were free of symptoms 60 d after intracranial injection were euthanized and examined.

## Bioluminescence imaging analysis of the intracranial gliomas

To monitor the growth of intracranial gliomas in living animal, we used bioluminescence imaging approach. We infected U87MG and U251 cells with a retroviral-based luciferase expression vector that also contains an internal ribosome entry site (IRES) and the hygromycin resistance gene. Hygromycin-resistant U87MG and U251 cells express a high level of luciferase (data not shown). These cells were then infected with retroviruses carrying the empty retroviral expression vector containing puromycin-resistant gene alone (U87MG/U251-Luc<sub>wt</sub>) or containing wild-type merlin (U87MG/U251-Luc<sub>merlin</sub>), merlinS518A (U87MG/U251-Luc<sub>merlinS518A</sub>), or merlinS518D (U87MG/U251-Luc<sub>merlinS518D</sub>). These double drug-resistant cells expressed high levels of luciferase and/or wt merlin/merlin mutant and were used for intracranial injection into Rag-1 mice. At 4, 10, and 16 d after the injections, bioluminescence images of the intracranial tumors were acquired by using IVIS-200 imaging system (Xenogen) at *In vivo* Molecular Imaging Shared Facility (Mount Sinai School of Medicine).

## Histology and immunohistochemistry

To determine the tumor cell proliferation rate *in vivo*, BrdUrd was injected i.p. into mice 4 h before euthanasia. Gliomas were removed, fixed, sectioned, and stained with H&E as described (13). In addition, the sections were reacted with anti-BrdUrd antibodies to detect proliferating cells or with the Apoptag kit to detect apoptotic cells *in situ* (14).

## Statistics

Other than the survival experiments, Student's *t* test was used to analyze statistical differences between the control and experimental groups. For the mouse survival experiments, log-rank statistical analysis (SigmaStat) was used to calculate the statistical differences between control and experimental groups. Differences were considered statistically significant at  $p < 0.05$ .

## Results

### Reduced NF2 expression in human gliomas

According to WHO classification, astrocytic tumors are classified and graded from 1 to 4 as follows: pilocytic astrocytoma (grade 1), diffuse astrocytoma (grade 2), anaplastic astrocytoma (grade 3), and glioblastoma multiforme (GBM; grade 4). We assessed the level of merlin expression in 23 human GBM tissues by Western blot and real-time qPCR analyses. Protein lysates from these 23 GBM samples were analyzed by Western blot using anti-merlin antibody (Santa Cruz; C-18), and merlin expression levels were determined by scanning densitometry (Gel-Pro). We observed more than a 2-fold reduction of merlin expression in 14 of 23 GBM tumors relative to normal brain (61%; Fig. 1A) and more than a 4-fold reduction in six tumors (26%; Fig. 1A). Real-time qPCR analysis of merlin RNA from the same 23 samples, as well as two normal brain (NB) and NHA samples, showed that, compared with NB and NHA cells, there is a >2-fold reduction of merlin RNA expression in 15 of 23 GBM tumors (65%; Fig. 1B) and more than a 4-fold reduction in 6 of these 23 samples (26%; Fig. 1B). The remaining tumors showed <2-fold decreases in merlin expression. Together, we found a 93% concordance between loss of merlin RNA and protein expression in these GBM tumors. In addition, using a glioma tissue microarray stained with NF2 (C-18) antibody, we observed that merlin expression was absent in 27.4% of the GBM tumors (Fig. 1C). Interestingly, we did not observe any reduction in merlin expression in anaplastic astrocytoma (WHO grade 3 tumors), suggesting that loss of merlin is associated with grade 4 glioma (GBM).

### Establishment of human glioma cells that overexpress merlin and merlin mutants

To assess the potential role of merlin in glioma growth, we first analyzed the level of merlin expression in a variety of human glioma cell lines. In general, human glioma cell lines, such as U87MG, U251, SF763, and SF767 that are capable of forming subcutaneous and/or intracranial tumors in immunodeficient Rag-1 mice, expressed lower levels of merlin and/or a phosphorylated/inactive form of merlin (lanes 12 and 20, the upper band of the double bands). In contrast, NHAs and the nontumorigenic or low tumorigenic human glioma cell lines, such as M089J, Hs683, LN18, SNB19, SF295, and SF210, expressed higher levels of merlin (Fig. 2A).

U87MG and U251 cells which express very low or intermediate levels of endogenous merlin, respectively, were infected with retroviruses containing the empty retroviral expression vector (U87MG/U251<sub>wt</sub>), wild-type merlin (U87MG/U251<sub>merlin</sub>), merlin S518A mutant (U87MG/U251<sub>merlinS518A</sub>), or merlinS518D mutant (U87MG/U251<sub>merlinS518D</sub>). The S518A mutation results in a non-phosphorylatable form of merlin that is constitutively active, whereas merlinS518D mimics a phosphorylated and inactive form of merlin (10,11,15). The retroviral expression vectors used also contain an IRES positioned between the cDNA inserts and the puromycin resistance gene, so that all the puromycin-resistant cells should express merlin or the merlin mutants. After selection of the infected cells with puromycin, the pooled drug-resistant cells were found to express high levels of merlin or the merlin mutants (Fig. 2B and Supplementary Fig. S1; data not shown). Glioma cells expressing exogenous merlin and merlinS518A, but not merlin S518D, displayed an altered morphology that is characterized by extended cellular processes and a reduced transformation phenotype (Fig. 2C; data not shown).

### Merlin reexpression inhibits anchorage-independent growth and invasiveness of glioma cells and sensitizes glioma cells to chemotherapy and irradiation

To determine how merlin affects the cellular behavior of glioma cells, we first investigated the effect of merlin on anchorage-independent growth of U87MG cells by assessing the ability of these transduced glioma cells to form colonies in soft agar. We found that U87MG<sub>wt</sub> and U87MG<sub>merlinS518D</sub> cells readily formed large colonies in soft agar and that merlin and

merlin<sub>S518A</sub> reexpression dramatically reduced the number and size of the colonies (Fig. 3A), suggesting that active, but not inactive, merlin inhibits anchorage-independent growth. This result is consistent with our previous findings (13). We then determined the effect of merlin on glioma cell invasion. Similarly, active, but not inactive, merlin inhibits invasiveness of these glioma cells (Fig. 3B).

Glioblastomas are often chemoresistant and radioresistant as a result of constitutive activation and/or induced activation of several distinct signaling pathways, including the phosphatidylinositol 3-kinase (PI3K) signaling pathway (16,17). We examined the ability of merlin to sensitize glioma cells to 5-FU and irradiation. We found that reexpression of merlin sensitized U87MG cells to 5-FU and irradiation (Fig. 3C and D). Whereas the exact mechanism underlying the slightly reduced apoptosis rate of U87MG<sub>wt</sub> cells treated with 20Gy of irradiation relative to those treated with 5 or 10Gy is not known, high dose radiation may actually induce a higher level of activation of antiapoptotic signals in U87MG<sub>wt</sub> cells, which counteracts the apoptotic effect of high-dose radiation (16,17). Regardless, reexpression of merlin consistently sensitizes the response of the U87 cells to radiation.

### **Merlin inhibits U87MG and U251glioma cell subcutaneous growth by reducing proliferation and promoting apoptosis *in vivo***

Transduced U87MG and U251 cells were used for subcutaneous tumor growth experiments to assess the effect of merlin and merlin mutants on tumor growth *in vivo*. We found that wild-type merlin and merlin<sub>S518A</sub>, but not merlin<sub>S518D</sub>, dramatically inhibited subcutaneous growth of glioma cells (Fig. 4A–C). To determine the cellular mechanism underlying this effect, we analyzed proliferation and apoptosis of the transduced U87MG cells *in vivo*. We observed that reexpression of merlin and merlin<sub>S518A</sub>, but not merlin<sub>S518D</sub>, inhibited tumor cell proliferation (BrdUrd incorporation) and promoted apoptosis (terminal deoxynucleotidyltransferase–mediated dUTP nick end labeling staining) of tumor cells *in vivo* (Fig. 4D).

### **Merlin inhibits the intracranial growth of U87MG and U251 glioma cells, whereas knockdown of merlin promotes U251 glioma intracranial growth**

To monitor intracranial tumor growth, we infected luciferase-expressing U87MG and U251 cells with the retroviruses carrying the empty retroviral expression vector containing puromycin-resistant gene alone (U87MG/U251-Luc<sub>wt</sub>), wild-type merlin (U87MG/U251-Luc<sub>merlin</sub>), merlin<sub>S518A</sub> (U87MG/U251-Luc<sub>merlinS518A</sub>), or merlin<sub>S518D</sub> (U87MG/U251-Luc<sub>merlinS518D</sub>). Transduced U87MG cells were injected intracranially into Rag-1 mice, and tumor growth was studied using the IVIS-200 imaging system (Xenogen; Fig. 5A). As seen with the subcutaneous explants, wild-type merlin and merlin<sub>S518A</sub>, but not merlin<sub>S518D</sub>, expression in either U87MG (Fig. 5B) or U251 (Fig. 5D) significantly increased the survival of the experimental mice. Importantly, a large fraction of these mice only had nonsymptomatic small tumors 40 days after intracranial injection. In contrast, the mean survival of the mice that received U87MG/U251-Luc<sub>wt</sub> and U87MG/U251-Luc<sub>merlinS518D</sub> cells was <3 to 4 weeks (Fig. 5B and D).

Unlike U87MG cells, which express very low levels of endogenous merlin (Fig. 2A, *lane 6, arrow*), U251 cells express intermediate levels of endogenous merlin (Fig. 2A, *lane 13, arrow*). Accordingly, U87MG cells grow more aggressively than U251 cells *in vivo* (Fig. 4 and Fig 5). To determine whether knockdown expression of endogenous merlin in U251 glioma cells promotes tumor growth, we screened a set of shRNAmir constructs against human merlin. A nontargeting shRNA construct was used as a negative control. The lentiviruses carrying these shRNA constructs were used to infect U251-Luc cells. We found that two of the three shRNAmir constructs (mer-shRNA#1 and mer-shRNA#3, Open Biosystems) reduced merlin

expression by ~70%, whereas the nontargeting control construct had no effect on merlin expression (Fig. 5C). We then assessed tumorigenicity of the pooled U251-Luc<sub>wt</sub>, U251-Luc<sub>mer-shRNA#1</sub>, U251-Luc<sub>mer-shRNA#3</sub>, and U251-Luc<sub>controlshRNA</sub> cells by injecting these cells intracranially into Rag1 mice. Consistent with our reexpression studies, knockdown of merlin expression in U251 cells increased intracranial glioma growth and reduced overall survival of these mice (Fig. 5D).

### Transcript profiling of U87MG<sub>merlin</sub> cells suggests that merlin is a master regulator of several important signaling pathways

To identify potential downstream targets of merlin glioma growth inhibition, we compared gene expression profiles from three independently transduced and pooled puromycin-resistant U87MG<sub>merlin</sub> and U87MG<sub>wt</sub> cells. We identified 362 genes whose expression increased and 364 genes whose expression decreased in U87MG<sub>merlin</sub> cells compared with U87MG<sub>wt</sub> cells (data not shown). These genes were then imported to David Functional Annotation Bioinformatics Microarray Analysis software<sup>4</sup> (NIAID/NIH) to enrich for functionally related gene groups affected by merlin expression. After classification of these transcripts into functional pathways, we found that merlin reexpression results in increased expression of transcripts that activate the Lats2 signaling pathway, as well as increased expression of molecules that inhibit canonical Wnt and RhoA signaling and decreased expression of transcripts that activate canonical Wnt and RhoA signaling (Supplementary Table S1).

### Merlin activates Lats2 signaling pathway and inhibits canonical and noncanonical Wnt signaling

To validate the microarray results, we performed quantitative real-time qPCR using cDNAs from U87MG<sub>merlin</sub> and U87MG<sub>wt</sub> cells. The qPCR results confirmed the increased expression of inhibitors of canonical Wnt signaling (DKK-1 and DKK-3) and decreased expression of an activator of canonical Wnt signaling (FZD1; Fig. 6A). In addition, we found that merlin reexpression reduced the expression of activators of RhoA signaling (ARHGEF3 and VAV3) and increased the expression of proteins that inhibit RhoA signaling (DLC1, ARHGAP29, and RRAD; Fig. 6A). Lastly, merlin reexpression resulted in increased expression of the mammalian homologues of proteins in the *Drosophila* Hippo (Hpo)–Warts (Wts)–Yorkie (Yki) pathway (FAT3, MST1, MST2, Lats1, and Lats2; Fig. 6A). Taken together, these results suggest that merlin activates Lats2 signaling and inhibits canonical and noncanonical Wnt signaling.

We next assessed these merlin-induced changes of the expression at the protein or functional level. Because canonical Wnt signaling regulates gene expression by modulating the levels of β-catenin expression, a coactivator of the TCF/LEF transcription factors, we performed reporter assays using a β-catenin–responsive luciferase reporter construct, TopFlash (Addgene). FopFlash, which contains mutated TCF/LEF binding sites, was used as a negative control. We found that β-catenin transcriptional activity is inhibited by wild-type merlin and merlinS518A, but not by merlinS518D (Fig. 6B). We then assessed RhoA activity in U87MG<sub>wt</sub> and U87MG<sub>merlin</sub> cells using a commercially available RhoA activity assay (Cytoskeleton, Inc.). We found that RhoA activity was reduced after wild-type merlin reexpression (data not shown).

We then used Western blotting to determine the activity and expression of several components of the Lats2 signaling cascade. Activation was assessed using phosphorylated-specific antibodies. We found that merlin reexpression resulted in increased phosphorylation of

<sup>4</sup><http://david.abcc.ncifcrf.gov/home.jsp>

MST1/2, Lats2, and YAP (Fig. 6D), whereas the levels of cIAP1/2 expression were reduced (Fig. 6D). These results show that merlin activates MST-Lats signaling in human glioma cells.

## Discussion

The *NF2* gene is a critical tumor suppressor for several distinct cell types in the nervous system, including Schwann and leptomeningeal cells, such that *Nf2* inactivation in Schwann cell precursors and leptomeningeal cells is sufficient for schwannoma and meningioma formation in mice, respectively. Because glial cell tumors (e.g., ependymomas) arise in patients with NF2, we postulated that merlin might also function as a negative growth regulator for glial cell tumors. In this study, we show for the first time that merlin expression at both the RNA and protein levels is decreased in sporadic glioblastoma tumors and malignant glioma cell lines. Moreover, we show that increased expression of merlin suppresses glioma cell growth *in vitro* and glioma tumor growth *in vivo* and that merlin knockdown promotes glioma tumor growth *in vivo*. Collectively, these findings suggest that merlin might be an important growth regulator in high-grade glioma and expand the role of the *NF2* gene in the pathogenesis of central nervous system tumors. *NF2* loss in GBM tumors is unlikely to result from mutational inactivation, in light of previous studies examining gliomas for *NF2* gene mutations (18). Moreover, we did not find reduced merlin expression in low-grade gliomas<sup>5</sup> or in WHO grade 3 gliomas, suggesting that reduced *NF2* expression might be a hallmark of grade 4 glioma.

In addition to its function as a potent negative growth regulator, we show that merlin also sensitizes glioma cells to 5-FU chemotherapy and irradiation. We show that merlin reexpression increased the response of U87MG cells to 5-FU. High-grade gliomas are often chemoresistant and radioresistant as a result of constitutive activation and/or induced activation of several distinct signaling pathways, including the PI3K signaling pathways (16,17). Irradiation activates PI3K pathway in human gliomas (16,17). In light of published reports in other tumor types (19,20), it is interesting to note that merlin reexpression results in decreased expression of two members of the cIAP family, cIAP1 and cIAP2. cIAP1 and cIAP2 have been shown to directly bind to and inhibit caspase activity (21), which underlies the prosurvival effect of IAP proteins. Studies have shown that both cIAP1 and cIAP2 are up-regulated in GBM tumors compared with normal brain tissue (data derived from ref. 22), suggesting a possible mechanism underlying the relative resistance of GBM tumors to chemotherapy and radiation.

In our studies, U87MG<sub>wt</sub> cells treated with 20 Gy of irradiation showed reduced apoptosis relative to U87MG cells treated with 5 or 10 Gy. Whereas these findings seem contradictory, high-dose radiation may actually induce a higher level of activation of antiapoptotic signals in U87MG<sub>wt</sub> cells, which counteracts the apoptotic effect of high-dose radiation (16,17). Regardless, reexpression of merlin consistently sensitizes the response of U87MG cells to radiation.

Numerous studies have focused on defining the mechanism underlying merlin tumor suppressor activity and identified several distinct growth regulatory pathways. One of these pathways includes the Rac1 signaling pathway. Merlin overexpression inhibits Rac1-mediated anchorage-independent growth (23) and inhibits the activity of the p21-activated kinase 1 (11). Related to this mechanism, a recent study showed that a GTP-binding protein (termed the NF2-associated GTP-binding protein) interacts with merlin and may regulate the antiproliferative activity of merlin by interfering with small GTPase protein signaling (24). In addition, other investigators have shown that merlin may regulate mitogen-activated protein kinase, Akt, and c-Jun NH<sub>2</sub> kinase signaling (15,25).

<sup>5</sup>S.S. Houshmandi and D.H. Gutmann, unpublished results.

These prior investigations have examined merlin in nonbrain tissues and tumors. To gain insights into the potential mechanism(s) responsible for merlin-negative regulation of brain tumor (GBM) growth, we performed RNA expression profiling. Our study revealed that merlin reexpression resulted in activation of the Lats signaling pathway and inhibition of canonical Wnt and non-canonical Wnt/RhoA signaling. These findings suggest that merlin may serve to integrate several signaling pathways important for cell growth, apoptosis, and motility in glioma cells.

In *Drosophila*, merlin (*mer*) inactivating mutations result in reduced apoptosis and increased cell proliferation, which led to the discovery that *mer* functions upstream of the Hpo-Wts-Yki pathway (26–29). In flies, FAT, a large protocadherin, functions upstream of merlin. Merlin activates Hpo kinase, which in turn phosphorylates and activates Wts kinase. Wts phosphorylates and inactivates Yki and blocks its proproliferation and antiapoptotic activity (26–31). Yki, a transcriptional coactivator, regulates the expression of a common set of downstream target genes, including wingless (*wg*), DIAP, and cyclin E (26–31).

The mammalian homologues of Hpo, Wts, Yki, DIAP, and *wg* are MST kinase 1/2 (32), Lats1/2 (33,34), YAP (35), cIAP1/2, and the Wnt family proteins. MST1 and MST2 can phosphorylate and activate Lats1 and Lats2 (36). Like MST1/2 genes, Lats1/2 genes encode serine/threonine kinases and display antitumor activity (37–39). Lats1 and Lats2 are downregulated in human astrocytomas through hypermethylation of their promoters (40). On the contrary, YAP is amplified in human cancers and displays oncogenic activity (35,41). As a transcriptional coactivator, YAP promotes cell proliferation and inhibits apoptosis by upregulating expression of cyclin E and cIAP1/2, respectively (28). Although it is unknown whether the entire FAT-Hpo-Wts-Yki signaling pathway is conserved in mammalian cells, like Yki, YAP rescues the pupal lethality caused by overexpression of *hpo* or *wts* in *Drosophila* (28). Similarly, human homologues of *hpo* and *wts* rescue their corresponding *Drosophila* mutants (42,43). In the current study, we show that merlin modulates the activity and/or expression MST1/2, Lats2, and YAP, suggesting that this pathway is conserved in glioma cells and is regulated by merlin. Our results also suggest that merlin inhibition of glioma cell proliferation and promotion of apoptosis may reflect the increased activation of MST1/2 and Lats1/2, which inhibits YAP activity, leading to reduced expression of cIAP1/2 and cyclin E (not shown).

Wnt signals play essential roles in regulating cell differentiation, proliferation, apoptosis, and motility (44). Wnts activate the canonical pathway by binding to the FZD receptors and the low-density lipoprotein receptor-related proteins (LRP-5 and LRP-6), which in turn activate  $\beta$ -catenin.  $\beta$ -Catenin interacts with members of the TCF/LEF family of transcription factors to induce expression of the Wnt-responsive genes (45). Antagonists of the Wnt signaling pathway include the members of the secreted frizzled-related protein family and the members of the Dickkopf family (46). Work in *Drosophila* implicated Wingless (Wg) as a downstream effector of merlin (29). Studies have shown that FDZ9 and WNT pathway are up-regulated in astrocytomas (47,48) and that DKK-1 sensitizes U87MG cells to apoptosis after alkylation agent induced DNA damage (49). Our finding that merlin reexpression in human glioma cells decreased FDZ1 expression, increased DKK1 and DKK3 expression, and reduced canonical Wnt activity is consistent with these observations.

Collectively, we show that merlin is a potent negative growth regulator in WHO grade 4 gliomas and that merlin reexpression results in decreased glioma cell growth *in vitro* and *in vivo*. We further showed that merlin induces apoptosis of glioma cells potentiated by chemotherapy and radiation. Analysis of the signaling pathways revealed that merlin regulates the MST/LATS/YAP/cIAP pathway, a critical modulator of apoptosis, and reduces canonical Wnt and RhoA signaling, important regulators of cell proliferation and/or motility. These novel

findings provide new insights into the pathogenesis of human high-grade gliomas and suggest new therapeutic strategies for these aggressive and typically fatal brain tumors.

## Supplementary Material

Refer to Web version on PubMed Central for supplementary material.

## Acknowledgments

**Grant support:** Department of Defense-U.S. Army Medical Research grants W81XWH-05-1-0191 (Q. Yu) and DAMD-17-04-0266 (D.H. Gutmann) and NIH NRSA fellowship grant 1F32CA128335-01A1 (S.S. Houshmandi).

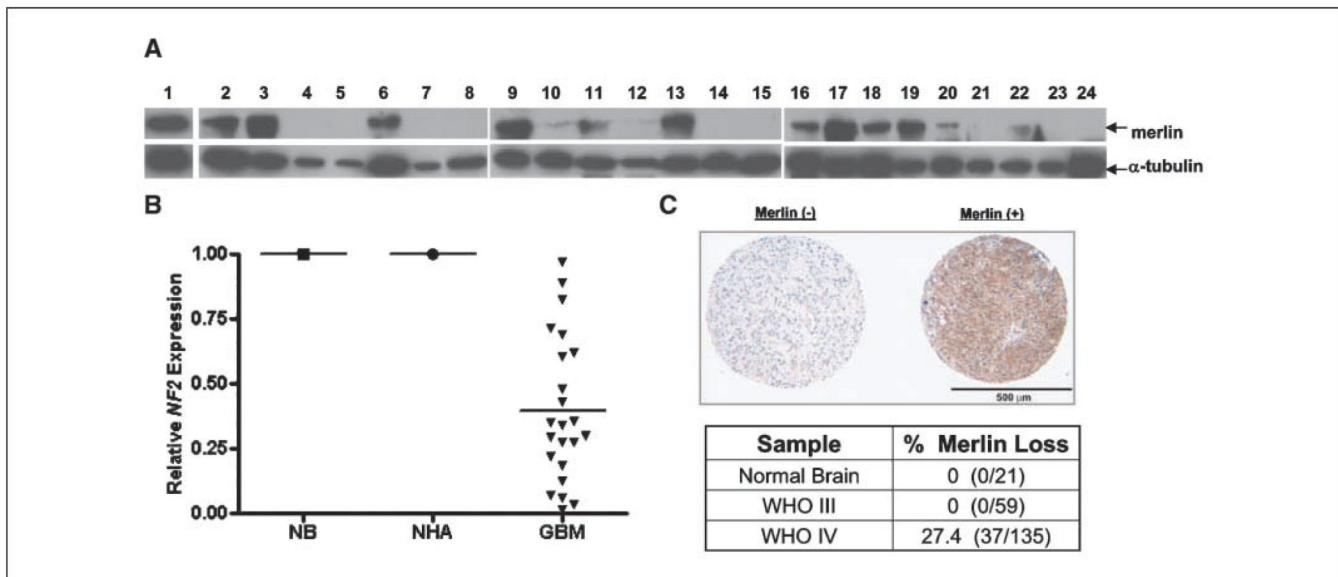
We thank Dr. Gregory Fuller (M. D. Anderson Cancer Center) for providing the glioma tissue microarray, Dr. Yu Zhou at the Molecular Imaging Shared Facility (Mount Sinai School of Medicine) for performing bioluminescence imaging analysis, Dr. John Tobias at the Bioinformatics Core of University of Pennsylvania for performing microarray analysis, and Dr. Stuart Aaronson and Dr. Ivan Stamenkovic for their stimulating discussions and support.

## References

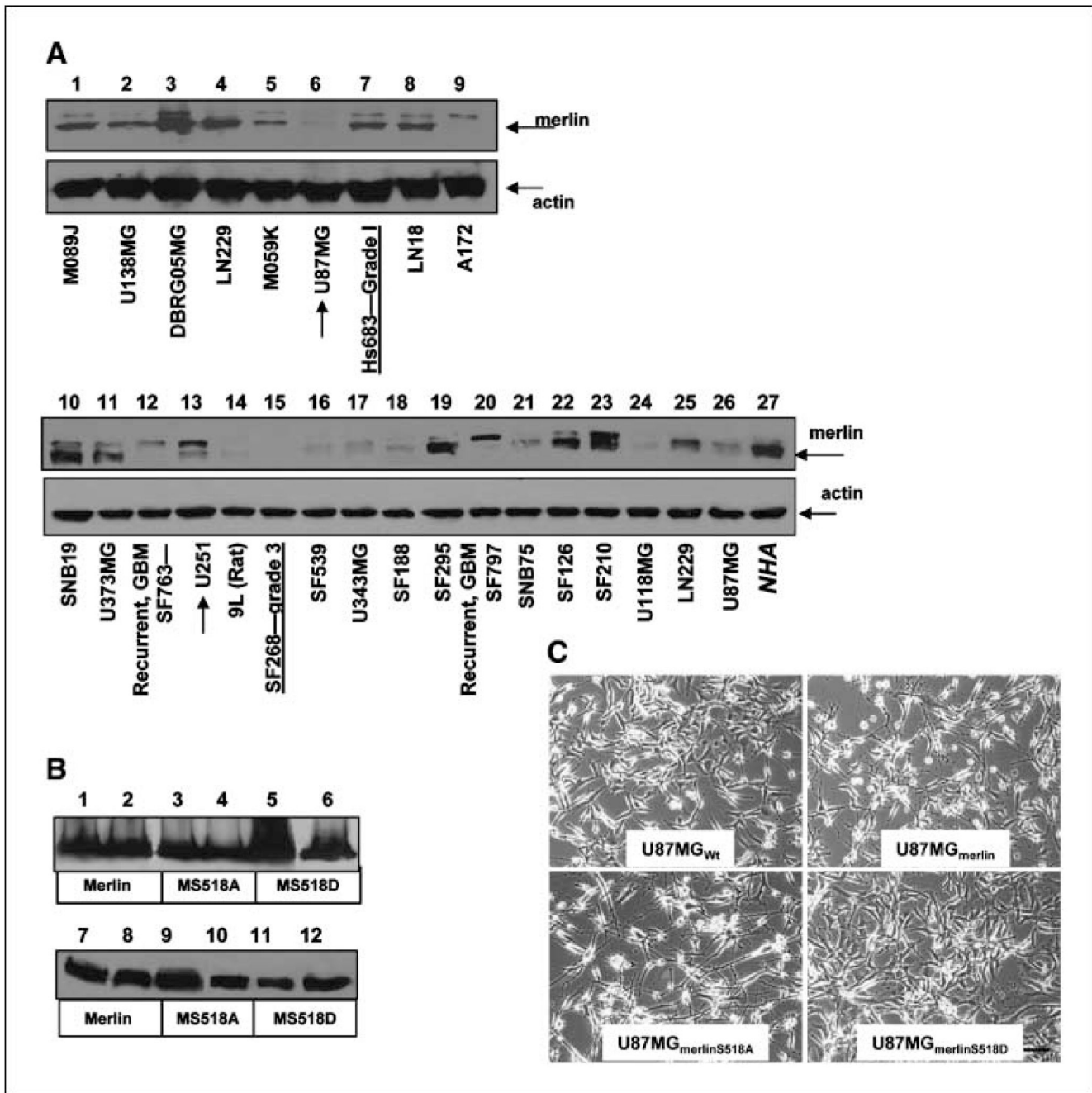
1. Maher EA, Furnari FB, Bachoo RM, et al. Malignant glioma: genetics and biology of a grave matter. *Genes Dev* 2001;15:1311–1333. [PubMed: 11390353]
2. Davis FG, Freels S, Grutsch J, Barlas S, Brem S. Survival rates in patients with primary malignant brain tumors stratified by patient age and tumor histological type: an analysis based on surveillance, epidemiology, and end results (SEER) data, 1973–1991. *J Neurosurg* 1998;88:1–10. [PubMed: 9420066]
3. Gutmann DH, Giordano MJ, Fishback AS, Guha A. Loss of merlin expression in sporadic meningiomas, ependymomas and schwannomas. *Neurology* 1997;49:267–270. [PubMed: 9222206]
4. Rouleau GA, Merel P, Lutchman M, et al. Alteration in a new gene encoding a putative membrane-organizing protein causes neurofibromatosis type 2. *Nature* 1993;363:515–521. [PubMed: 8379998]
5. Trofatter JA, MacCollin MM, Rutter JL, et al. A novel moesin-, ezrin-, radixin-like gene is a candidate for the neurofibromatosis 2 tumor suppressor. *Cell* 1993;72:1–20.
6. Bretscher A, Chambers D, Nguyen R, Reczek D. ERM-Merlin and EBP50 protein families in plasma membrane organization and function. *Annu Rev Cell Dev Biol* 2000;16:113–143. [PubMed: 11031232]
7. Gautreau A, Louvard D, Arpin M. ERM proteins and NF2 tumor suppressor: the Yin and Yang of cortical actin organization and cell growth signaling. *Curr Opin Cell Biol* 2002;14:104–109. [PubMed: 11792551]
8. McClatchey AI. Merlin and ERM proteins: unappreciated roles in cancer development? *Nat Rev Cancer* 2003;3:877–883. [PubMed: 14668818]
9. Bianchi AB, Hara T, Ramesh V, et al. Mutations in transcript isoforms of the neurofibromatosis 2 gene in multiple human tumour types. *Nat Genet* 1994;6:185–192. [PubMed: 8162073]
10. Sherman L, Xu H-M, Geist RT, et al. Interdomain binding mediates tumor growth suppression by the NF2 gene product. *Oncogene* 1997;15:2505–2509. [PubMed: 9395247]
11. Kissil JL, Wilker EW, Johnson KC, Eckman MS, Yaffe MB, Jacks T. Merlin, the product of the Nf2 tumor suppressor gene, is an inhibitor of the p21 activated kinase, Pak1. *Mol Cell* 2003;12:841–849. [PubMed: 14580336]
12. Houshmandi SS, Surace EI, Zhang HB, Fuller GN, Gutmann DH. Tumor suppressor in lung cancer-1 (TSLC1) functions as a glioma tumor suppressor. *Neurology* 2006;67:1863–1866. [PubMed: 17130425]
13. Bai Y, Liu YJ, Wang H, Xu Y, Stamenkovic I, Yu Q. Inhibition of the hyaluronan-CD44 interaction by merlin contributes to the tumor-suppressor activity of merlin. *Oncogene* 2007;26:836–850. [PubMed: 16953231]
14. Liu YJ, Xu Y, Yu Q. Full-length ADAMTS-1 and the ADAMTS-1 fragments display pro- and antimetastatic activity, respectively. *Oncogene* 2006;25:2452–2467. [PubMed: 16314835]

15. Tang X, Jang SW, Wang X, et al. Akt phosphorylation regulates the tumour-suppressor merlin through ubiquitination and degradation. *Nat Cell Biol* 2007;9:1199–1207. [PubMed: 17891137]
16. Park CM, Park MJ, Kwak HJ, et al. Ionizing radiation enhances matrix metalloproteinase-2 secretion and invasion of glioma cells through Src/epidermal growth factor receptor-mediated p38/Akt and phosphatidylinositol 3-kinase/Akt signaling pathways. *Cancer Res* 2006;66:8511–8519. [PubMed: 16951163]
17. Kao GD, Jiang Z, Fernandes AM, Gupta AK, Maity A. Inhibition of phosphatidylinositol-3-OH kinase/Akt signaling impairs DNA repair in glioblastoma cells following ionizing radiation. *J Biol Chem* 2007;282:21206–21212. [PubMed: 17513297]
18. Alonso ME, Bello MJ, Arjona D, et al. Analysis of the NF2 gene in oligodendrogiomas and ependymomas. *Cancer Genet Cytogenet* 2002;134:1–5. [PubMed: 11996787]
19. Liu X, Shi Y, Giranda VL, Luo Y. Inhibition of the phosphatidylinositol 3-kinase/Akt pathway sensitizes MDA-MB468 human breast cancer cells to cerulenin-induced apoptosis. *Mol Cancer Ther* 2006;5:494–501. [PubMed: 16546963]
20. Belyanskaya LL, Hopkins-Donaldson S, Kurtz S, et al. Cisplatin activates Akt in small cell lung cancer cells and attenuates apoptosis by survivin upregulation. *Int J Cancer* 2005;117:755–763. [PubMed: 15981204]
21. Aggarwal BB, Bhardwaj U, Takada Y. Regulation of TRAIL-induced apoptosis by ectopic expression of antiapoptotic factors. *Vitam Horm* 2004;67:453–483. [PubMed: 15110190]
22. Bredel M, Bredel C, Juric D, et al. Functional network analysis reveals extended gliomagenesis pathway maps and three novel MYC-interacting genes in human gliomas. *Cancer Res* 2005;65:8679–8689. [PubMed: 16204036]
23. Shaw RJ, Paez JG, Curto M, et al. The Nf2 tumor suppressor, merlin, functions in Rac-dependent signaling. *Dev Cell* 2001;1:63–72. [PubMed: 11703924]
24. Lee H, Kim D, Dan HC, et al. Identification and characterization of putative tumor suppressor NGB, a GTP-binding protein that interacts with the neurofibromatosis 2 protein. *Mol Cell Biol* 2007;27:2103–2119. [PubMed: 17210637]
25. Chadee DN, Xu D, Hung G, et al. Mixed-lineage kinase 3 regulates B-Raf through maintenance of the B-Raf/Raf-1 complex and inhibition by the NF2 tumor suppressor protein. *Proc Natl Acad Sci U S A* 2006;103:4463–4468. [PubMed: 16537381]
26. Hamaratoglu F, Willecke M, Kango-Singh M, et al. The tumour-suppressor genes NF2/Merlin and Expanded act through Hippo signalling to regulate cell proliferation and apoptosis. *Nat Cell Biol* 2006;8:27–36. [PubMed: 16341207]
27. McCartney BM, Kulikauskas RM, LaJeunesse DR, Fehon RG. The neurofibromatosis-2 homologue, Merlin, and the tumor suppressor expanded function together in *Drosophila* to regulate cell proliferation and differentiation. *Development* 2000;127:1315–1324. [PubMed: 10683183]
28. Huang J, Wu S, Barrera J, Matthews K, Pan D. The Hippo signaling pathway coordinately regulates cell proliferation and apoptosis by inactivating Yorkie, the *Drosophila* homolog of YAP. *Cell* 2005;122:421–434. [PubMed: 16096061]
29. Pellock BJ, Buff E, White K, Hariharan IK. The *Drosophila* tumor suppressors expanded and merlin differentially regulate cell cycle exit, apoptosis, and wingless signaling. *Dev Biol* 2007;304:102–115. [PubMed: 17258190]
30. Cho E, Feng Y, Rauskolb C, Maitra S, Fehon R, Irvine KD. Delineation of a Fat tumor suppressor pathway. *Nat Genet* 2006;38:1142–1150. [PubMed: 16980976]
31. Maitra S, Kulikauskas RM, Gavilan H, Fehon RG. The tumor suppressors merlin and expanded function cooperatively to modulate receptor endocytosis and signaling. *Curr Biol* 2006;16:702–709. [PubMed: 16581517]
32. Creasy CL, Chernoff J. Cloning and characterization of a member of the MST subfamily of Ste20-like kinases. *Gene* 1995;167:303–306. [PubMed: 8566796]
33. Aylon Y, Michael D, Shmueli A, Yabuta N, Nojima H, Oren M. A positive feedback loop between the p53 and Lats2 tumor suppressors prevents tetraploidization. *Genes Dev* 2006;20:2687–2700. [PubMed: 17015431]

34. Takahashi Y, Miyoshi Y, Takahata C, et al. Downregulation of LATS1 and LATS2 mRNA expression by promoter hypermethylation and its association with biologically aggressive phenotype in human breast cancers. *Clin Cancer Res* 2005;11:1380–1385. [PubMed: 15746036]
35. Overholtzer M, Zhang J, Smolen GA, et al. Transforming properties of YAP, a candidate oncogene on the chromosome 11q22 amplicon. *Proc Natl Acad Sci U S A* 2006;103:12405–12410. [PubMed: 16894141]
36. Chan EH, Nousiainen M, Chalamalasetty RB, Schafer A, Nigg EA, Sillje HH. The Ste20-like kinase Mst2 activates the human large tumor suppressor kinase Lats1. *Oncogene* 2005;24:2076–2086. [PubMed: 15688006]
37. Li Y, Pei J, Xia H, Ke H, Wang H, Tao W. Lats2, a putative tumor suppressor, inhibits G1/S transition. *Oncogene* 2003;22:4398–4405. [PubMed: 12853976]
38. St John MA, Tao W, Fei X, et al. Mice deficient of Lats1 develop soft-tissue sarcomas, ovarian tumours and pituitary dysfunction. *Nat Genet* 1999;21:182–186. [PubMed: 9988269]
39. McPherson JP, Tamblyn L, Elia A, et al. Lats2/Kpm is required for embryonic development, proliferation control and genomic integrity. *EMBO J* 2004;23:3677–3688. [PubMed: 15343267]
40. Jiang Z, Li X, Hu J, et al. Promoter hypermethylationmediated down-regulation of LATS1 and LATS2 in human astrocytoma. *Neurosci Res* 2006;56:450–458. [PubMed: 17049657]
41. Zender L, Spector MS, Xue W, et al. Identification and validation of oncogenes in liver cancer using an integrative oncogenomic approach. *Cell* 2006;125:1253–1267. [PubMed: 16814713]
42. Wu S, Huang J, Dong J, Pan D. hippo encodes a Ste-20 family protein kinase that restricts cell proliferation and promotes apoptosis in conjunction with salvador and warts. *Cell* 2003;114:445–446. [PubMed: 12941273]
43. Tao W, Zhang S, Turenhchalk GS, et al. Human homologue of the *Drosophila melanogaster* lats tumour suppressor modulates CDC2 activity. *Nat Genet* 1999;21:177–181. [PubMed: 9988268]
44. Vlad A, Röhrs S, Klein-Hitpass L, Müller O. The first five years of the Wnt targetome. *Cell Signal*. 2007 Nov 17;[Epub ahead of print]
45. Moon RT, Kohn AD, De Ferrari GV, Kaykas A. WNT and  $\beta$ -catenin signaling: diseases and therapies. *Nat Rev Genet* 2004;5:691–701. [PubMed: 15372092]
46. Kawano Y, Kypta R. Secreted antagonists of the Wnt signaling pathway. *J Cell Sci* 2003;116:2627–2634. [PubMed: 12775774]
47. Zhang Z, Schittenhelm J, Guo K, et al. Up-regulation of frizzled 9 in astrocytomas. *Neuropathol Appl Neurobiol* 2006;32:615–624. [PubMed: 17083476]
48. Jozwiak J, Kotulska K, Grajkowska W, et al. Upregulation of the WNT pathway in tuberous sclerosis-associated subependymal giant cell astrocytomas. *Brain Dev* 2007;29:273–280. [PubMed: 17071037]
49. Shou J, Ali-Osman F, Multani AS, Pathak S, Fedi P, Srivenugopal KS. Human Dkk-1, a gene encoding a Wnt antagonist, responds to DNA damage and its over-expression sensitizes brain tumor cells to apoptosis following alkylation damage of DNA. *Oncogene* 2002;21:878–889. [PubMed: 11840333]

**Figure 1.**

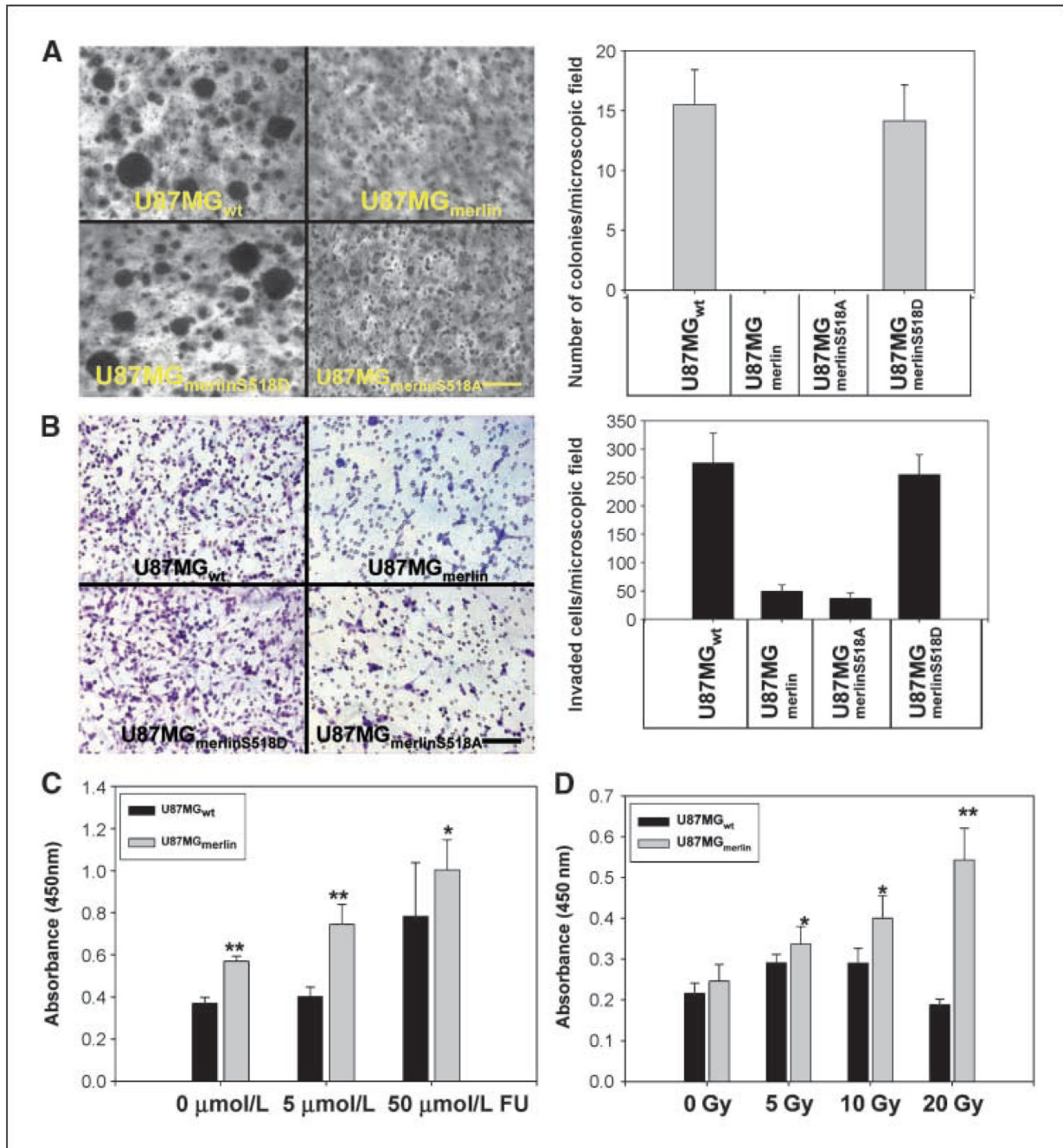
Expression of merlin is down-regulated in human GBM samples. *A*, merlin expression in NB (*lane 1, top*) and human gliomas (*lanes 2–24, top*) was determined by Western blotting using anti-merlin antibody (C-18, Santa Cruz). Tubulin was included as an internal control for equal protein loading (*bottom*). *B*, merlin mRNA expression was examined by real-time qPCR using human merlin primers in the same GBM samples used in the Western blotting as well as NB and NHA samples. *C*, merlin immunohistochemistry was performed on normal brain and gliomas representing WHO malignancy grades 3 and 4. Representative immunohistochemistry images are shown (*top*). Whereas no loss of merlin expression was observed in normal brain and anaplastic astrocytomas (*WHO III*), >27% of glioblastomas (*WHO IV*) exhibited loss of merlin expression (*bottom*).



**Figure 2.**

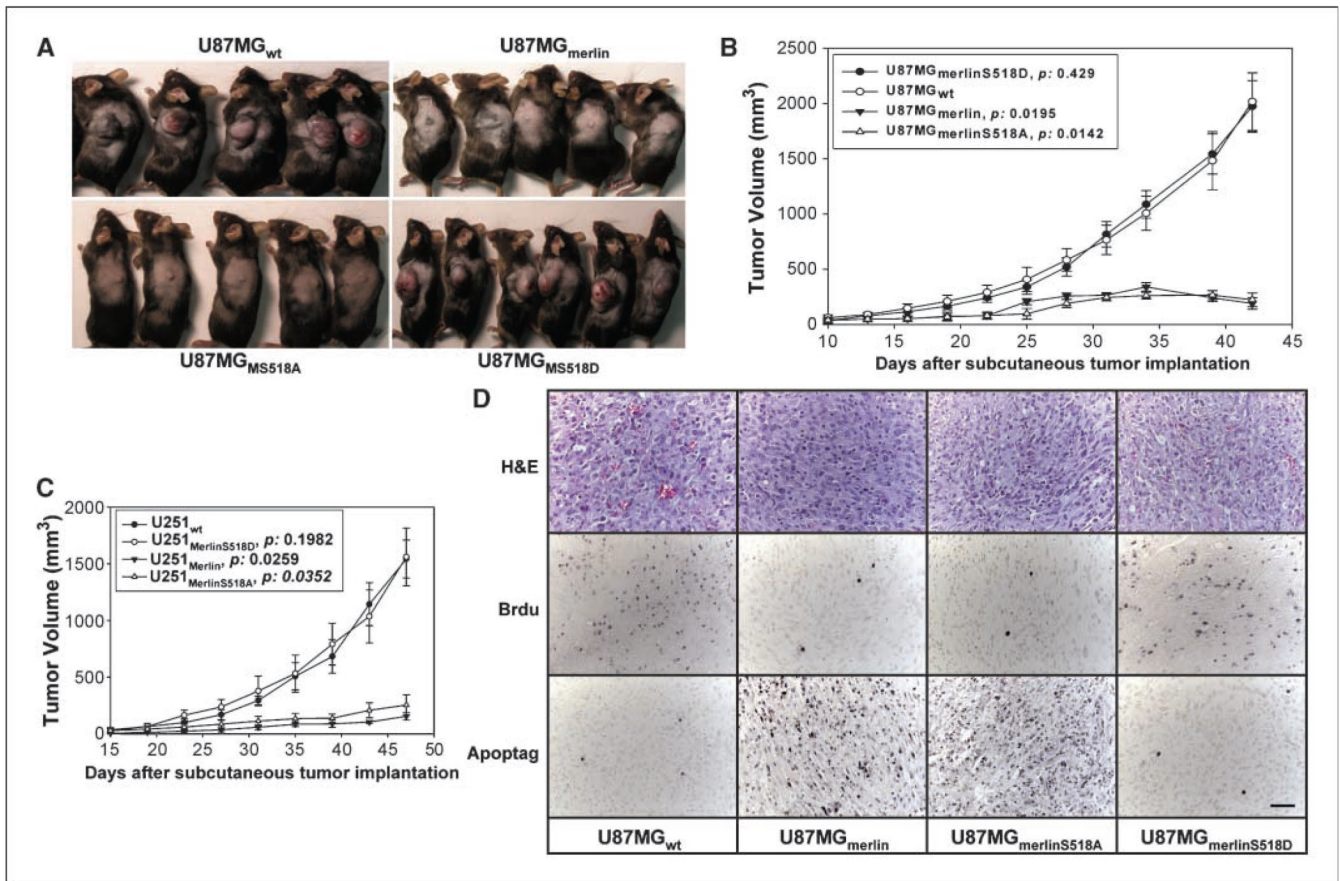
**Establishment of glioma cells expressing merlin and merlin mutants.** *A*, expression of endogenous merlin in a panel of human/rat glioma cells was determined by Western blotting using anti-merlin antibody (C-18, Santa Cruz), including M089J, U138MG, DBRG05MG, LN229, M059K, U87MG (*lane 6, A*), Hs683, LN18, and A172 cells (*A, top, lanes 1–9*; ATCC), SNB19, U373MG, SF763, U251 (*lane 13*), 9L (rat, *lane 14*), SF268, SF539, U343MG, SF188, SF295, SF797, SNB75, SF126, SF210, U118MG, LN229, U87MG, and NHAs (ALLCELLS, Inc.; *A, bottom, lanes 10–27*, UCSF and NCI collections). Total protein (50 µg) was loaded in each lane. The WHO grades 1 and 3 glioma cells are indicated. All the other glioma cells are derived from grade 4 GBM tumors. *B*, U87MG/U251<sub>merlin</sub>, U87MG/U251<sub>merlinS518A</sub>, and

U87MG/U251<sub>merlinS518D</sub> cells express a similar level of v5-epitope tagged exogenous merlin and the merlin mutants as determined by Western blot using anti-v5 mAb (Invitrogen). *Lanes 1–6*, the proteins derived from the transduced U87MG cells; *lanes 7–12*, the proteins derived from the transduced U251 cells. Total protein (20 µg) was loaded in each lane. *C*, transduced U87MG cells ( $2 \times 10^5$  per dish) were seeded in 35-mm cell culture dishes and grown for 24 h before taking photographs. U87MG<sub>merlin</sub> and U87MG<sub>merlinS518A</sub> cells display an altered morphology when compared with U87MG<sub>wt</sub> and U87MG<sub>merlinS518D</sub> cells. *Bar*, 120 µm.

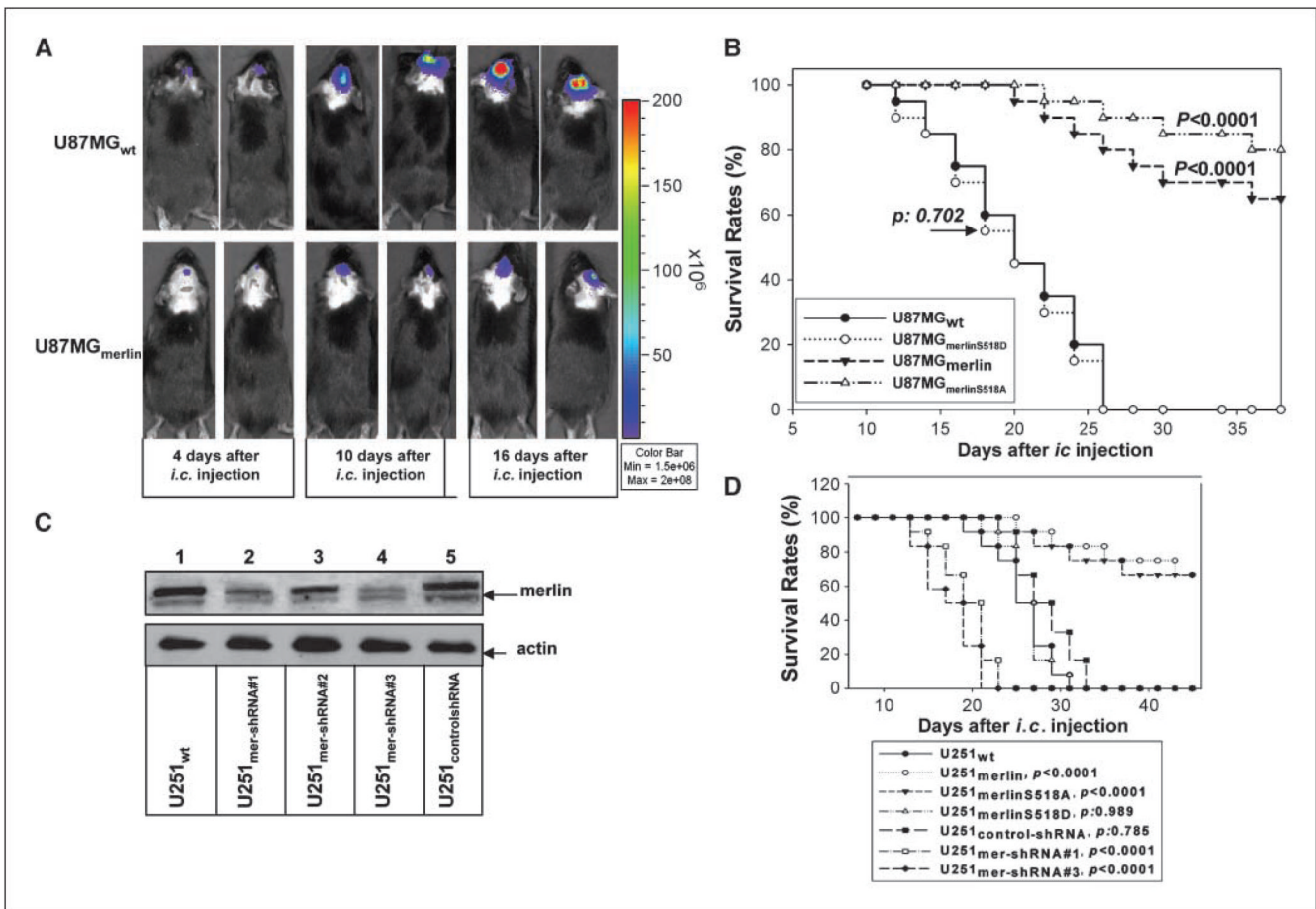
**Figure 3.**

Increased expression of merlin alters U87MG cell growth (anchorage independent), motility, and response to chemotherapy and radiation. **A**, reexpression of merlin and merlinS518A, but not merlinS518D, inhibited anchorage-independent growth of U87MG cells. Three weeks after seeding the cells in soft agar, 30 randomly selected microscopic fields were counted.

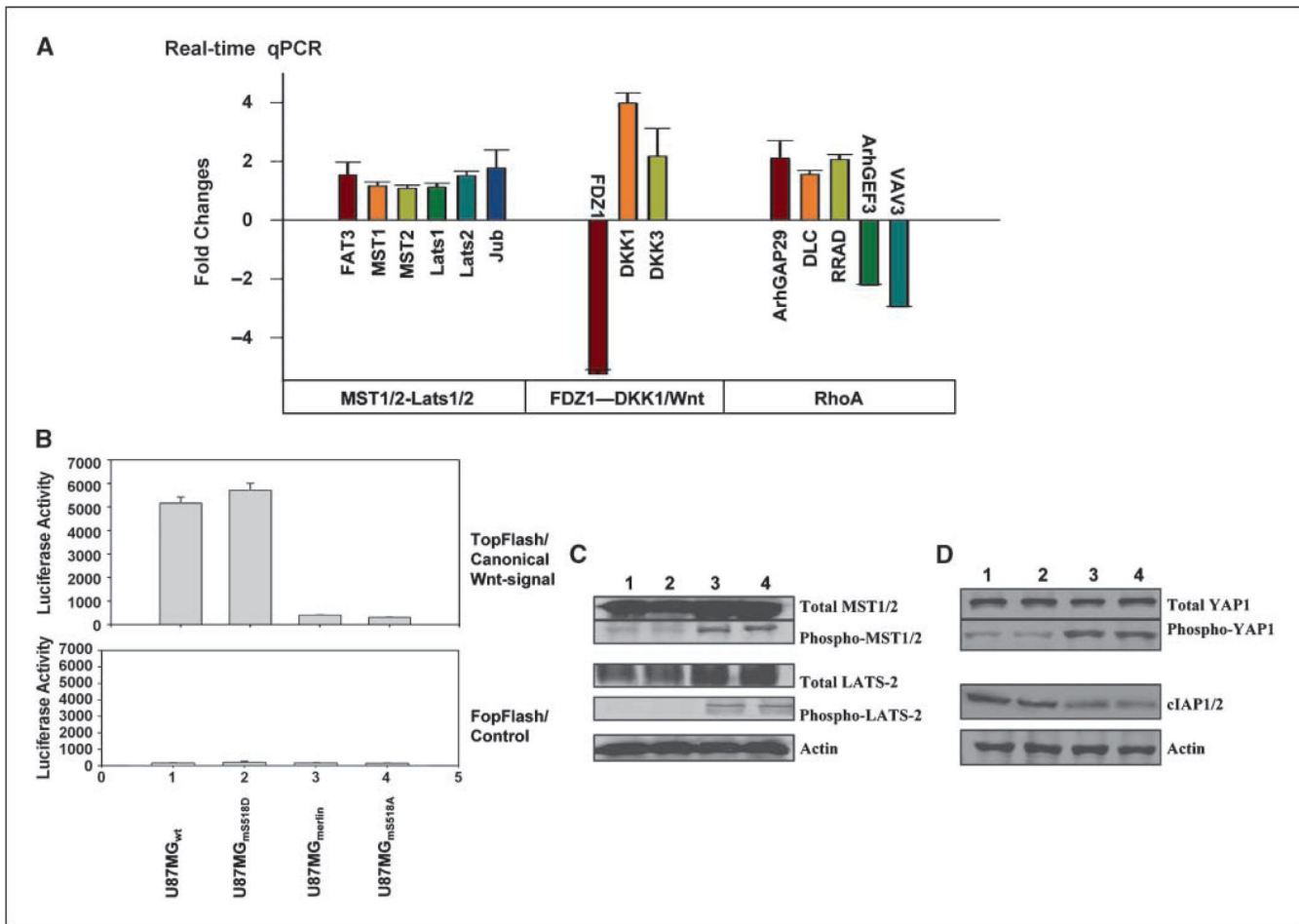
*Columns*, mean; *bars*, SD. *Bar*, 480 μm. **B**, reexpression of merlin and merlinS518A, but not merlinS518D, inhibited U87MG cells invasion through Matrigel. Quantitation is shown in the graph to the right of the photomicrographs. Thirty randomly selected microscopic fields were counted. *Scale bar*, 200 μm. Reexpression of merlin promoted drug-induced (**C**) and radiation-induced (**D**) apoptosis of U87MG<sub>wt</sub> cells.

**Figure 4.**

Merlin reexpression potently inhibits U87MG and U251 subcutaneous tumor growth. *A*, Photographs of U87MG<sub>wt</sub>, U87MG<sub>merlinS518A</sub>, U87MG<sub>merlin</sub>, and U87MG<sub>merlinS518D</sub> subcutaneous tumors. *B* and *C*, growth rates of the subcutaneous tumors derived from the transduced U87MG and U251 cells were determined as described in Materials and Methods and expressed as the mean of tumor volume ( $\text{mm}^3$ )  $\pm$  SD. The *P* values demonstrating significant inhibition are included. *D*, morphology, proliferation, and apoptosis of explanted glioma tumors. Tumor sections were stained with H&E to determine histologic morphology. *In vivo* proliferation was detected using an anti-BrdUrd antibody (Roche). Apoptosis *in situ* was detected using the Apoptag kit (Chemicon). Tumor sections are derived from U87MG<sub>wt</sub>, U87MG<sub>merlin</sub>, U87MG<sub>merlinS518A</sub>, and U87MG<sub>merlinS518D</sub>. Bar, 100  $\mu\text{m}$ .

**Figure 5.**

Merlin inhibits U87MG and U251 glioma intracranial growth, whereas merlin knockdown promotes U251 glioma intracranial growth. *A*, bioluminescence imaging analysis of mice 4, 10, and 16 d after the intracranial injection of U87MG-Luc<sub>wt</sub> (*top*) and U87MG-Luc<sub>merlin</sub> (*bottom*). The images were obtained 4 min after injection of D-luciferin using the same intensity scaling. *B* and *D*, survival rates of mice after the intracranial injections of transduced U87MG (*B*) and U251 (*D*) cells. The *P* values demonstrating significant effects on survival are included. *C*, knockdown of merlin expression in U251 cells. Western blot was performed using the anti-merlin antibody (C-18, Santa Cruz) on lysates from U251-Luc<sub>wt</sub>, U251-Luc<sub>mer-shRNA#1</sub>, U251-Luc<sub>mer-shRNA#2</sub>, U251-Luc<sub>mer-shRNA#3</sub>, and U251-Luc<sub>controlshRNA</sub> cells.

**Figure 6.**

Merlin activates Lats2 signaling and inhibits canonical Wnt and RhoA signaling in glioma cells. *A*, real-time qPCR validation of the microarray results. *B*, luciferase activity was measured in U87MG<sub>WT</sub>, U87MG<sub>merlin</sub>, U87MG<sub>merlinS518D</sub>, and U87MG<sub>merlinS518A</sub> cells 24 h after transfection of cells with TopFlash (*top*) or FopFlash (*bottom*). *C* and *D*, Western blots were performed on lysates from U87MG<sub>WT</sub> (*lanes 1 and 2*) and U87MG<sub>merlin</sub> (*lanes 3 and 4*) cells using the antibodies (as detailed in the figure) against MST1/2 (*C*, Bethyl Laboratories), Lats2 (*C*, Bethyl Laboratories), YAP (*D*, Abnova), cIAP1/2 (*D*, Santa Cruz), and actin (*C* and *D*, Sigma) and the antibodies against phosphorylated MST1/2 (*C*, Cell Signaling), phosphorylated Lats2 (*C*, Abnova), and phosphorylated YAP (*D*, Cell Signaling).